Title
Effects of fluoroquinolones and tetracyclines on mitochondria of human retinal MIO-M1 cells

Authors
Salimiaghdam, Nasim
Singh, Lata
Schneider, Kevin
et al.

Publication Date
2022

DOI
10.1016/j.exer.2021.108857

Peer reviewed

HHS Public Access

Author manuscript

Exp Eye Res. Author manuscript; available in PMC 2023 February 23.

Published in final edited form as:

Exp Eye Res. 2022 January ; 214: 108857. doi:10.1016/j.exer.2021.108857.

Effects of fluoroquinolones and tetracyclines on mitochondria of human retinal MIO-M1 cells

Nasim Salimiaghdam[a,1], **Lata Singh**[a,b], **Kevin Schneider**[a], **Marilyn Chwa**[a], **Shari R. Atilano**[a], **Angele Nalbandian**[a], **G. Astrid Limb**[c], **M. Cristina Kenney**[a,d,*]

[a]Department of Ophthalmology, Gavin Herbert Eye Institute, University of California Irvine, Irvine, CA, 92697, USA

[b]Department of Pediatrics, All India Institute of Medical Sciences, New Delhi, India

[c]Institute of Ophthalmology, University College, London, United Kingdom

[d]Department of Pathology and Laboratory Medicine, University of California Irvine, Irvine, CA, 92697, USA

Abstract

Our goal was to explore the detrimental impacts of ciprofloxacin (CPFX) and tetracycline (TETRA) on human retinal Müller (MIO-M1) cells *in vitro*. Cells were exposed to 30, 60 and 120 μg/ml of CPFX and TETRA. The cellular metabolism was measured with the MTT assay. The JC-1 and CM-H2DCFDA assays were used to evaluate the levels of mitochondrial membrane potential (MMP) and ROS (reactive oxygen species), respectively. Mitochondrial DNA (mtDNA) copy number, along with gene expression levels associated with apoptotic (*BAX, BCL2-L13, BCL2, CASP-3* and *CASP-9*), inflammatory (*IL-6, IL-1β, TGF-α, TGF-β1* and *TGF-β2*) and antioxidant pathways (*SOD2, SOD3, GPX3* and *NOX4*) were analyzed via Quantitative Real-Time PCR (qRT-PCR). Bioenergetic profiles were measured using the Seahorse® XF Flux Analyzer. Cells exposed 24 h to 120 μg/ml TETRA demonstrated higher cellular metabolism compared to vehicle-treated cells. At each time points, (i) all TETRA concentrations reduced MMP levels and (ii) ROS levels were reduced by TETRA 120 μg/ml treatment. TETRA caused **(i)** higher expression of *CASP-3, CASP-9, TGF-α, IL-1B, GPX3* and *SOD3* but **(ii)** decreased levels of *TGF-B2* and *SOD2*. ATP production and spare respiratory capacity declined with TETRA treatment. Cellular metabolism was reduced with CPFX 120 μg/ml in all cultures and

*Corresponding author. Gavin Herbert Eye Institute, Director of Mitochondria Research Laboratory, University of California Irvine, Department of Ophthalmology, 843 Health Science Rd., Hewitt Hall, Room 2028, Irvine, CA, 92697, USA. mkenney@hs.uci.edu (M.C. Kenney).

[1]NS is an Arnold and Mabel Beckman Retinal Degeneration Fellow.

Authors' contributions

Nasim Salimiaghdam planned the study, designed experiments, wrote the manuscript, and analyzed data. Lata Singh and Angele Nalbandian edited the manuscript. Cristina Kenney developed the concepts, edited the manuscript, provided resources for the study. Astrid Limb provided the MIO-M1 cell lines. Kevin Shneider, Marilyn Chwa and Shari Atilano contributed with designing and performing some of the experiments.

Conflicts of interest/disclosures

None.

Patients and public involvement statement

Patients or the public were not involved in the design, or conduct, or reporting, or dissemination plans of our research.

60 μg/ml after 72 h. The CPFX 120 μg/ml reduced MMP in all cultures and ROS levels (72 h). CPFX treatment **(i)** increased expression of *CASP-3, CASP-9*, and *BCL2-L13*, **(ii)** elevated the basal oxygen consumption rate, and **(iii)** lowered the mtDNA copy numbers and expression levels of *TGF-B2*, IL-6 and IL-1B compared to vehicle-control cells. We conclude that clinically relevant dosages of bactericidal and bacteriostatic antibiotics can have negative effects on the cellular metabolism and mitochondrial membrane potential of the retinal MIO-M1 cells *in vitro*. It is noteworthy to mention that apoptotic and inflammatory pathways in exposed cells were affected significantly This is the first study showing the negative impact of fluoroquinolones and tetracyclines on mitochondrial behavior of human retinal MIO-M1 cells.

Keywords

MIO-M1 cells; Antibiotics; Bactericidal; Bacteriostatic

1. Introduction

Antibiotics have saved millions of lives by preventing and treating a myriad of infectious diseases. Fluoroquinolones are bactericidal antibiotics with a broad spectrum of activity. They can be classified into four generations based on the range of their activity (Sharma et al., 2009; Mohammed et al., 2019; Vila et al., 1996). Norfloxacin and ciprofloxacin are two antibiotics administered by topical, intravitreal and systemic routes for ocular infections such as endophthalmitis (Mather et al., 2002; Smith et al., 2001). Their mechanisms of action are through the direct inhibition of DNA gyrase and topoisomerase IV, which are vital enzymes in the DNA synthesis process (Hooper, 2001).

In general, fluoroquinolones are well tolerated medications. However, some individuals have significant adverse effects including optic neuropathy, cardiac arrhythmias, hypomania, and hypoglycemia (Falagas et al., 2007; Samarakoon et al., 2007; Kanbay et al., 2006; Sarkar et al., 2013). Between 2000 and 2007, Etminan and colleagues conducted a case control study among 989,591 Canadian patients with usage of oral fluoroquinolones. Retinal detachment after fluoroquinolone use was identified in 4384 (3.3%) cases of participants, demonstrating a small but real risk for patients using these antibiotics (Etminan et al., 2012). Tetracyclines (e.g. tetracycline, doxycycline and minocycline) are bacteriostatic antibiotics with activity against a wide array of gram positive and gram-negative bacteria (Roberts, 2019). These antibiotics interact with the bacterial protein synthesis processes by reversibly binding to the libosomal 30s subunit, which blocks the binding of the mRNA-ribosome complex to the aminoacyle-tRNA acceptor site (Shutter and Akhondi, 2019). They also have anti-inflammatory properties and have been used at low doses to improve inflammatory diseases such as sarcoidosis, scleroderma and ocular rosacea (Sapadin and Fleischmajer, 2006; Salamon, 1985). Tetracyclines chelate ZN^{2+} leading to inhibition of matrix metalloproteinase activity. Side effects of the different types of tetracyclines including interference of bone growth and oral mucosa (Sánchez et al., 2004; Smilack et al., 1991). Wallace et al. validated the significant reduction of aqueous humor and intraocular pressure in rabbits after one day of intravitreal administration of tetracycline derivatives (Wallace, 1989).

Mitochondria are intracellular organelles found in large numbers in metabolically active cells and play critical roles in respiration, energy production, apoptosis, production of reactive oxygen species (ROS) and retrograde signaling to the nucleus. Mitochondria originated from endosymbiotic bacteria (a-proteobacteria) (Cavalier-Smith, 2006). Hence, mitochondria have remarkable structural and functional similarities to bacteria, including their circular DNA, libosomal subunits, the invagination of membrane and their sizes (Andersson et al., 2003). *In vitro* studies have reported negative effects of antibiotics on the mitochondria of various cell lines. For example, Beberok et al. demonstrated that the U87MG cell line (human glioblastoma) treated with moxifloxacin and ciprofloxacin (0.001, 0.005, 0.01, 0.05, 0.1, 0.5 and 1.0 μmol/ml) for 24, 48 and 72 h had decreased mitochondrial membrane potential, which in turn activated the intrinsic mitochondrial pathway and induced cellular apoptosis (Beberok et al., 2018). Remarkably, this negative association may be most important in the elderly population that suffer from age-related macular degeneration (AMD), since damaged mitochondria are often found in these disorders (Kenney et al., 2010). The Müller cells (retinal glial cells) along with retinal pigment epithelial (RPE) cells are main mediators of inflammatory chemokines in retinal inflammatory conditions (Natoli et al., 2017a). Human retinal Müller (MIO-M1) cells are a spontaneously immortalized Müller cell line that retains morphological and molecular features characteristics of primary cells *in vitro* (Limb et al., 2002). Many drug studies in transformed cell lines are not able to truly recapitulate functions of primary cells (i.e., cell proliferation). Previous studies performed on cultured MIO cells of vertebrate retina demonstrated that these cells are highly proliferative and capable of expressing dopaminergic characteristics of neurons (Kubrusly et al., 2008). They exhibits progenitor characteristics and may express markers of post mitotic retinal neurons as well as S-opsins (Hollborn et al., 2011). Previous studies demonstrated the capability of retinal Müller cells in phenotype transformation as neuronal stem cells, which has a role regarding specific retinopathic changes. Valez et al. concluded that during retinal detachment, the alteration of MIO-M1 cells phenotype affected by ARPE-19 cells, facilitated the pathogenicity of proliferative vitreoretinopathy (Velez et al., 2012). Notably, there are studies validated the promotion of inflammation by retinal Müller cells, considering their role in expressing chemokines induced by IL-1β (Natoli et al., 2017b). Lorenz and colleagues the considerable impacts of retinal Müller cells as potential antigen presenting cells in the course of ocular neuroinflammation conditions (Lorenz et al., 2021). Our recent ARPE-19 cell study demonstrated that CPFX and TETRA treatment induced negative impacts such as reduction of mitochondrial membrane potential and cellular metabolism. Also, CPFX treatment caused significant higher expression of inflammatory (*IL-6*) and apoptotic (*BAX, BCL2-L13, CASP-7* and *CASP-9*) genes (Salimiaghdam et al., 2020).

In this study, we investigated the potential harmful effects of the ciprofloxacin (CPFX) and tetracycline (TETRA) on the mitochondria and the cellular health in human retinal Müller cells.

2. Materials and methods

2.1. Cell culture

Müller cells (MIO-M1) were provided by the Dr. G Astrid Limb Laboratory (Institute of Ophthalmology, UCL, London) and grown in a mixture (D-MEM) (1X) (Dulbecco's Modified Eagle's medium/nutrient mixture) (Invitrogen, Carlsbad, CA), 4500 mg/L D-glucose, 110 mg/L sodium pyruvate, 10% fetal bovine serum, 0.58% L-glutamine, antibiotics (streptomycin sulfate 0.1 mg/ml, penicillin G 100 U/ml and gentamycin 10 mg/ml) and 10 mM non-essential amino acids. Incubation was performed in standard conditions (95% humidity, 5% CO2 at 37 °C).

Treatment concentrations of CPFX (Cat#17850, Sigma-Aldrich, St. Louis, MO) or TETRA (Cat# 87128, Sigma-Aldrich) were 0, 30, 60 and 120 μg/ml. Exposure periods were 24, 48 and 72 h 0.1 N solution of hydrochloric acid (HCl) and methanol (Meth) were used as the vehicles for CPFX and TETRA, respectively. Also, they are considered as control groups in all the experiments.

2.2. Cell metabolism (MTT assay)

The MTT assay was performed for the evaluation of metabolism levels. MIO-M1 cells were cultured in 96-well plates (10^4/well). After adding 10μl MTT assay reagent (3-(4,5-Dimethyltiazol-2-yl)-2,5-dipheniltetrazolium bromide; Catalog# 30006, Biotium, CA), incubation at 37 °C for 2 h was completed. After adding 100 μl of DMSO to each well, the plates were analyzed (signal at 570nm and reference at 630nm) with the absorbance reader (Biotek Elx808 Absorbance Reader, Winooski, VT). For the MTT experiments, there were four CPFX groups (vehicle-treated (HCl or Meth), CPFX 30 μg/ml, 60 μg/ml or 120 μg/ml) and four TETRA groups (vehicle-treated (HCl or Meth), 30 μg/ml, 60 μg/ml and 120 μg/ml). Each of the groups had 12 wells per treatment and the entire experiment was repeated four times.

2.3. Mitochondria membrane potential (MMP)

Cells were cultured and treated in 96-well plates for 24, 48 and 72 h. The JC-1 reagent (5,5′,6,6′- tetrachloro1,1′,3,3′-tetraethyl-benzimidaz olylcarbocyanine iodide; Catalog# 30001, Biotium, CA) was added to each well. Plates were read via the fluorescent plate reader at green (EX 485 nm and EM 535 nm) and red (EX 550 nm and EM 600 nm) emissions to determine the ratios of red to green fluorescence (SoftMax Pro, version 6.4, Catalog# 94089, Sunnyvale, CA, USA). For these experiments, there were four CPFX groups (vehicle-treated (HCl or Meth), CPFX 30 μg/ml, 60 μg/ml or 120 μg/ml) and four TETRA groups (vehicle-treated (HCl or Meth), 30 μg/ml, 60 μg/ml and 120 μg/ml). Each of the groups had 12 wells per treatment and the entire experiment was repeated four times.

2.4. Reactive oxygen species (ROS) assay

Cells were seeded in 96-well plates (10^4/well) and the H_2DCFDA solution (2′, 7′-dichlorhydrofluorescin diacetates; Catalog# D399, Thermo Fisher Scientific, Waltham, MA) was added to each well. This dye is converted into a fluorescent molecule in the presence of ROS. Finally, the plates were read at excitation (EX, 492nm) and emission (EM, 520nm)

wavelengths using the fluorescent plate reader (SoftMax Pro, version 6.4, Catalog# 94089, Sunnyvale, CA).). For the ROS experiments, there were four CPFX groups (vehicle-treated (HCl or Meth), CPFX 30 μg/ml, 60 μg/ml or 120 μg/ml) and four TETRA groups (vehicle-treated (HCl or Meth), 30 μg/ml, 60 μg/ml and 120 μg/ml). Each of the groups had 12 wells per treatment and the entire experiment was repeated four times.

2.5. RNA and DNA isolation and cDNA amplification

MIO-M1 cells were cultured with 120 μg/ml concentrations of CPFX and TETRA in 6 well plates for 48 h. Then, the RNeasy Mini-Extraction kit (Qiagen, Inc.) and Pure Genomic DNA Mini Kit (Thermo Fisher Scientific, Inc., Cat#K1820-01) were used for the isolation of RNA and DNA, respectively, from the cell lysates, based on the manufacture's protocol. Briefly, quantifications of the isolated RNA and DNA were performed via Nano Drop 1000 (Thermo-Scientific). Superscript IV VILO Master Mix with ezDNase Enzyme (ThermoFisher) was used for the reverse transcription of each isolated RNA sample to complementary DNA (cDNA).

2.6. Quantitative real time polymerase chain reaction (qRT-PCR)

Total RNA was isolated from cultured untreated cells (n = 3), CPFX-treated (n = 3) or TETRA treated samples (n = 3) and the corresponding vehicle-treated (HCl, Meth) cultures (n = 3). All target primers were predesigned KiCqStart SYBR® Green primers (Sigma–Aldrich) or Qiagen QuantiTect Primer Assays and are listed in Table 1. The evaluation of relative expression of genes associated with pro-inflammatory (*TGF-α, TGF-β1, TGF-β2, IL-6* and *IL-1β*), antioxidant enzymes (*NOX4, GPX3, SOD2* and *SOD3*) and pro-apoptotic (*CASP3, BCL2-L13, BAX* and *CASP9* (mitochondria specific)), and anti-apoptotic (*BCL2*) pathways were conducted via qRT-PCR using the PowerUp SYBR Green Master Mix (ThermoFisher, USA) on a ThermoFisher Quant Studio 3 Real-Time PCR System. In the purine salvage pathway, *HPRT1* is a housekeeping enzyme that recycles guanine and inosine. *HPRT1* has been used as an endogenous control for molecular studies investigating changes in gene expression as a housekeeping gene. To standardize expression levels for all primers, the *HPRT1* primer, as a reliable endogenous control, was selected as the reference gene (Hollborn et al., 2011; Asiabi et al., 2020; Silver et al., 2006). We used the $^{\Delta\Delta}$Ct method to analyze data: in which $^{\Delta}$Ct = [Ct (threshold value) of the target gene] − [Ct for HPRT1], and $^{\Delta\Delta}$Ct = $^{\Delta}$Ct of the treatment condition − $^{\Delta}$Ct of the untreated condition. The fold changes of treated conditions compared to untreated condition were calculated as: fold change = $2^{-\Delta\Delta Ct}$. Analyses were done in triplicates. Analyses were performed for the untreated and also the vehicle-control (HCl, Meth) samples versus the antibiotic treated (CPFX, TETRA) samples.

2.7. Mitochondrial DNA (mtDNA) copy number assay

The total DNA was isolated from the untreated samples, vehicle-control (HCl, Meth) wells (n = 3) and treated (CPFX, TETRA) cells (n = 3). Then, the quantitative measurement of mtDNA was performed by TaqMan Gene Expression assay (Thermo Fisher Scientific, USA). By comparing the levels of mitochondrial DNA copy number (MT-ND2) versus nuclear DNA (18S), the relative levels of mtDNA copy numbers were assessed. Analyses were done in triplicates.

2.8. Biogenetic profile and oxygen consumption rate

For measuring the oxygen consumption rate (OCR), we used the Seahorse XF24 flux analyzer (Seahorse Bioscience/Agilent, Santa Clara, CA). This measures the extracellular acidification rate (ECAR) for glycolysis, ATP production, basal respiration, maximal respiration, proton leak, non-mitochondrial respiration spare respiratory capacity and oxygen consumption rate (Fig. 7a). Cells were cultured and treated in 96 well plates (80,000/well). Samples incubated overnight under 5% CO2 in 37 °C. Plates were washed and 500 μl of the unbuffered DMEM (Dulbecco's modified Eagle's medium, pH 7.4) was added with the supplements of 10 mM sodium pyruvate (Invitrogen-Molecular Probes, Carlsbad, CA), 17.5 mM Glucose (Sigma, St Louis, MO) and 200 mM L-glutamine (Invitrogen-Molecular Probes). Then there was the sequentially addition of 1μM Oligomycin (ATP synthase inhibitor), 1μM of FCCP (a chemical uncoupler and inducer of maximal respiration) followed by 1 μM Rotenone and Antimycin A (RO/AA) (inhibitors of electron transport chain). The RIPA lysis buffer (Millipore, Billerica, MA) containing phosphatase arrest (G-Biosciences, St. Louis, MO) and protease inhibitor (Sigma, St. Louis, MO) were used for protein isolation. Qubit buffer was mixed with the isolated protein and Qubit 2.0 fluorometer (Invitrogen, Grand Island, NY) was used to measure protein levels, which were used for normalization of obtained data of each well.

For data analyses of bioenergetic profiles, we used the XF Reader software from Seahorse Bioscience. The OCR is determined by measuring the drop of O2 partial pressure over time followed by linear regression to find the slope. The data were exported to GraphPad Prism (Version 5.0, GraphPad Software, Inc., and San Diego, CA).

2.9. Statistical analyses

Statistical analyses were performed using GraphPad Prism (Version 5.0, GraphPad Software, Inc., and San Diego, CA). The one-way ANOVA followed by Tukey post hoc test was performed when comparing differences between the untreated group, the vehicle-control cells (HCl and Meth) groups and the antibiotic-treated (CPFX, TETRA) groups. A statistically significant P value was considered less than 0.05. Performing gene expression and mtDNA copy number, there were 3 replicates for each treatment modality. Gene expression and mtDNA copy number for each condition was analyzed in triplicate.

3. Results

3.1. Cellular metabolism

There are trends of decreased cell metabolism with CPFX treatment. In 24 and 48 h cultures, cellular metabolism of cells exposed to 120 μg/ml CPFX declined significantly ($p < 0.05$; Fig. 1a). Also, after 72 h incubation, cells treated with 60 μg/ml ($p < 0.01$; Figs. 1a) and 120 μg/ml CPFX ($p < 0.0001$; Fig. 1a) showed reduced levels of cellular metabolism compared to vehicle-treated group. In contrast, samples exposed to TETRA showed different results. In 24 h cultures, the highest concentration of TETRA increased cellular metabolism ($p < 0.01$; Fig. 1d), but there was no significant impact of TETRA at other time periods or concentrations. These results demonstrate that there is a negative association between

cellular metabolism of MIO-M1 cells and CPFX. However, the higher concentration of TETRA induced increase of cellular metabolism.

3.2. Changes in mitochondrial membrane potential (MMP)

There was a declining pattern of MMP in CPFX-treated cells, it reached significance in cells treated with 120 μg/ml CPFX after 24 h ($p < 0.05$; Figs. 1b), 48 h ($p < 0.05$; Figs. 1b) and 72 h ($p < 0.0001$; Fig. 1b). In all time periods, exposure to 60 and 120 μg/ml TETRA caused significant decrease of the MMP ($p < 0.0001$; Fig. 1e). Also, MMP in 24, 48 and 72 h cultures treated with TETRA 30 μg/ml showed remarkable reduction of MMP in comparison with vehicle-control samples ($p < 0.01$; Fig. 1e), ($p < 0.05$; Fig. 1e) and ($p < 0.01$; Fig. 1e), respectively. Altogether, these results show that over time, both antiobiotics can affect MMP of MIO-M1 cells in a negative way.

3.3. ROS production

There were no statistically significant alterations in ROS levels in 24 and 48 h cultures exposed to CPFX compared to vehicle-treated samples. However, in 72 h cultures, cells treated with 120 μg/ml CPFX showed a remarkable declined in ROS level (Fig. 1c). In comparison with vehicle-treated samples, the levels of ROS were reduced significantly in cells treated with 120 μg/ml TETRA for 24 ($p < 0.01$; Figs. 1f), 48 h ($p < 0.05$; Figs. 1f) and 72 h ($p < 0.05$; Fig. 1f). Altogether, these results suggest that higher treatment concentrations of TETRA cause a reduction of ROS levels.

3.4. Significant reduction of mtDNA copy numbers

In CPFX-treated MIO-M1 cells, the relative ratio of mtDNA copy numbers diminished significantly compared to vehicle-treated group ($p < 0.01$; Fig. 2). There was no significant effect of TETRA on mtDNA copy number levels in the treated MIO-M1 cells. This result demonstrates that CPFX could potentially lead to a significant reduction of mtDNA copy numbers.

3.5. Expression levels for pro-inflammatory, antioxidant and proapoptosis genes

Table 1 provides information of genes of interest in MIO-M1 cells treated with CPFX and TETRA compared to vehicle-control cells in this study. In the CPFX-treated cultures, the pro-inflammatory genes were expressed at significantly lower levels for *TGF-β2* ($p < 0.0001$; Fig. 3c), *IL-6* ($p < 0.05$; Fig. 3d) and *IL-1β* ($p < 0.0001$; Fig. 3e) compared to vehicle-control samples. Treatment with TETRA induced higher expression levels of *TGF-a* ($p < 0.01$; Fig. 3a) and *IL-1β* ($p < 0.01$; Fig. 3e) compared to vehicle-control cells. However, after treatment with TETRA, there was a reduced expression level of *TGF-β2* ($p < 0.05$; Fig. 3c).

In the TETRA-treated cells, there were higher expression levels of *GPX3* ($p < 0.05$; Fig. 4b) and *SOD3* ($p < 0.0001$; Fig. 4d), but the expression level of *SOD2* was signficantly decreased ($p < 0.0001$; Fig. 4c). Treatment with CPFX did not alter the gene expression levels for *NOX4, GPX3, SOD2* or *SOD3* compared to vehicle-treated cultures (Fig. 4a-d).

When the apoptotic pathway was evaluated, *CASP-3* showed higher expression levels with both CPFX ($p < 0.01$; Fig. 5a) and TETRA ($p < 0.01$; Fig. 5a) compared to vehicle-treated cells. Moreover, *CASP-9* ($p < 0.0001$; Fig. 5b) and *BCL2-L13* ($p < 0.01$; Fig. 5d) genes had higher expression levels in CPFX-treated MIO-M1 cells, compared to HCl-treated groups. Also, there was an increased expression level of *CASP-9* gene ($p < 0.05$; Fig. 5b) in TETRA treated group compared to vehicle-control cells.

Interestingly, there were no changes in the expression levels of *TGF-a* (Fig. 3a), *TGF-β1* (Fig. 3b), *NOX4* (Fig. 4a), *GPX3* (Fig. 4b), *SOD2* (Fig. 4c), *SOD3* (Fig. 4d), *BCL2* (Fig. 5c) and *BAX* (Fig. 5e) after treatment with CPFX. In addition, TETRA-treatment had no effects on expression levels of the *TGF-β1* (Fig. 3b), *IL-6* (Fig. 3d), *NOX4* (Fig. 4a), *BCL2* (Fig. 5c) and *BCL2-L13* (Fig. 5d) compared to the vehicle-treated cells. Fig. 6 represents a summary of the gene expression after treatment with CPFX and TETRA.

3.6. Biogenetic profile and oxygen consumption rate

Fig. 7a represents the rate of mitochondrial respiration over time in treated cells after the sequential injections. Basal respiration indicates the energetic demand of the cell under base line conditions and the level of oxygen consumption to meet the cellular ATP demand. In the baseline condition, cells treated with CPFX showed increased level of OCR ($p < 0.01$; Fig. 7b) compared to vehicle-control group. In the TETRA-treated cultures, there was a significant reduction of ATP production compared to vehicle-control group ($p < 0.05$; Fig. 7c). Moreover, the spare respiratory capacity, which is an indicator of cellular capability, declined significantly in TETRA-treated cells compared to vehicle-control cells ($p < 0.05$; Fig. 7d).

These results demonstrate that CPFX and TETRA have an effect on the bioenergetic profile of treated MIO-M1 cells.

4. Discussion

Fluoroquinolones are bactericidal agents with potential broad-spectrum activities that are classified into four groups. Studies have shown that the systemic fluoroquinolones have adverse ocular effects including diplopia, iris trans-illumination, pigment dispersion, uveitis, optic neuropathy, retinal hemorrhage, and retinal detachment (Etminan et al., 2012). The significance of testing the effectiveness of new potent antibiotics for monotherapy has increased due to retinal toxicity induced by treatment of exogenous bacterial endophthalmitis with multiple antibiotics (Stevens et al., 1991; Thompson, 2007). The toxicity of fluoroquinolones in the eyes tends to be dose-dependent and caused by class effects and complex fluoroquinolone structures (Thompson, 2007). One group suggested that exposure of the iris to light may affect the toxicity of fluoroquinolones simply by increasing its tissue-binding affinity (Sandhu et al., 2016).

MMP was measured using JC-1 dye, which is specific and sensitive to MMP reduction but it is poorly water soluble and has a low signal-to-background ratio (Perry et al., 2011). In the present study, we showed that MIO-M1 cells treated with CPFX showed: **(i)** significant reduction of cellular viability and MMP at the highest CPFX concentration

in all cultures; **(ii)** higher expression of *BCL-2-L13, CASP-3*, and *CASP-9;* and **(iii)** lower expression levels of *IL-6, IL-1B*, and *TGF-B2*, along with decreased mtDNA copy numbers. The TETRA-treated MIO-M1 cells showed **(i)** significantly lower MMP levels with 30, 60 and 120 μg/ml concentrations at all time periods; **(ii)** increased expression *of CASP-3, CASP-9, TGF-α, IL-1B, GPX3* and *SOD3;* and **(iii)** decreased expression levels of *TGF-β2* and *SOD2* compared to vehicle-control cells. The findings suggest that clinically relevant concentrations of TETRA and CPFX may indeed have negative effects on the MIO-M1 cells.

Also, in our study, CPFX treated cells had higher basal level oxygen consumption rates compared to vehicle-control treated cells, while the treatment with TETRA did not elicit a change. After the injection of Oligomycin, which inhibits the ATP synthase, the TETRA exposed cells showed lower production of ATP. Moreover, spare respiratory capacity declined in cells treated with TETRA compared to vehicle-control samples. Therefore, TETRA treatment has negative impacts on cellular flexibility and response to stress with respect to the ATP production process. It is noteworthy that the changes in bioenergetic profiles differed between CPFX and TETRA treatments. Using Seahorse XF extracellular flux analyzer, Lobritz et al., showed the induction of physiological changes by bacteriostatic and bactericidal antibiotics at the level of cellular respiration in *E. coli* and *S. aureus*. The study demonstrated that growth inhibition caused by bacteriostatic antibiotics is linked to cellular respiration and metabolism deceleration (Lobritz et al., 2015). Dijk et al., examined the role of mitochondria and potential of doxycycline in combination with gemcitabine in adenocarcinoma cell line A549 ρ° and cultured fibroblasts. After treatment with doxycycline, A549 cells showed a decrease of mitochondrial-encoded proteins, respiration and membrane potentials, and an increase of reactive oxygen species, but without changing the level of cellular ATP (Dijk et al., 2020). Therefore, these studies suggest that measurement of mitochondrial respiration can reflect reliable information of mitochondrial functions including metabolic status, ATP generation, oxygen consumption rates, and affected mitochondria complex units in MIO cells.

There are studies showing that both bactericidal (ciprofloxacin) and bacteriostatic (tetracycline) antibiotics disrupt mitochondrial function in mammalian cells, leading to oxidative stress and damage (Kalghatgi et al., 2013a). Previous studies have also shown that antibiotic treatment can damaged mammalian cells, but these results were shown at concentrations considerably higher than those applied in clinical practice (Lawrence et al., 1996; Duewelhenke et al., 2007). Patients with reduced antioxidant defense system or those who are genetically predisposed to mitochondrial dysfunction disease are more susceptible to bactericidal antibiotics. Identifying fluoroquinolones as a cause of ROS overproduction and mitochondrial dysfunction in mammalian cells provides a basis for developing therapeutic strategies that could help alleviate adverse side effects associated with antibiotics (Hangas et al., 2018; Barnhill et al., 2012).

Both the production of ROS and mitochondrial damage are related to phototoxicity of retina. While both may cause apoptosis, the order in which they occur is debatable (Glickman, 2002). Prior literature demonstrates that the fluoroquinolones have cytotoxic and apoptosis-inducing properties. Kalghatgi et al. reported that 10 μg/ml ciprofloxacin

causes mitochondrial dysfunction and overproduction of ROS in mammalian cells (Kalghatgi et al., 2013b). Kohanski and colleagues evaluated the impacts of three different bacteriocidal antiobiotics including B-lactam (5 μg/ml ampicillin), aminoglycoside (5 μg/ml kanamycin) and quinolones (250 ng/ml norfloxacin) on mitochondria and formation of ROS in comparison with four categories of bacteriostatic agents (macrolide erythromycin, chloramphenicol, tetracycline and spectinomycin) *Escherichia coli*. The authors concluded that although bacteriocidals induced oxidative cellular death by formation of hydroxyl radicals, bacteriostatics did not stimulate ROS production (Kohanski et al., 2007). Wagai and Tawara (1992) also reported that the ROS are generated in solutions of quinolones under UV-A irradiation (Wagai and Tawara, 1992).

Müller cell (GFAP positive) activation and inflammatory response in the whole retina of mitochondrial impaired (Ndufs4 KO mice) were reported, suggesting mitochondrial damage can provoke significant responses in in Müller cells in vivo. The treatment of either CPFX or TETRA induced increased expression levels of pro-inflammatory cytokines (Jiang et al., 2019). CM-H2DCFDA or DCFH dye was used to measure ROS in our study. This dye is also used to monitor redox signaling changes in cells in response to oxidative stimulus but it is unstable, and once excited with laser, it is easily activated even without ROS induction. It is important to remember these limitations when interpreting data collected with the H2DCFDA probe (Kalyanaraman et al., 2012). In the present study, the highest treatment concenteration of TETRA (120 μg/ml) decreased ROS levels after 24 h. Also, there were varying expression levels of antioxidant enzyme genes affected by TETRA treatment.

Furthurmore, TETRA treatment induced significantly higher expression levels of *CASP-3* and *CASP-9* (pro-apoptosis), *SOD3* and *GPX3* (antioxidant enzymes), and *TGF-a* and *IL-1B* (inflammatory) related genes. CPFX exposure stimulated higher expression of the *BCL2-L13*, *CASP-3* and *CASP-9* (pro-apoptotsis genes), along with significant reduction of mtDNA copy number levels. We found that MMP was significantly reduced in TETRA-treated cultures at all time periods, while the MMP was lower significantly only in the 120 μg/ml CPFX cultures. These findings suggest that both antiobiotics could affect MMP in cultured MIO-M1 cells in a negative way over time. Our findings are in agreement with zebrafish studies showing histopathological and toxicological side effects of varying concentrations (45, 60 and 90 mg/L) of two tetracyclines (β-diketone antibiotics-DKAs) and fluoroquinolones that included reduction and deepening of mitochondrial cristae and mitochondrial swelling over 7, 14 and 21 days (Ding et al., 2017).

5. Conclusion

We conclude that a clinically relevant dosage of bacteriocidal and bacteriostatic antiobiotics have negative impacts on retinal MIO-M1 cells *in vitro*. These results may be critical in populations affected by specific age-related diseases, such as AMD, Alzheimer's disease and Parkinson's disease, which already have damaged mitochondria. Further clinical trials and in vivo investigations are needed to determine if these antibiotics may be contributing to additional mitochondrial dysfunction.

Acknowledgment

We would like to acknowledge our appreciation to our colleagues who participated in this study.

Funding

This work was supported by the Discovery Eye Foundation, Polly and Michael Smith, Edith and Roy Carver, Iris and B. Gerald Cantor Foundation, Max Factor Family Foundation, and NEI R01 EY027363 (MCK). Supported in part by an Unrestricted Departmental Grant from Research to Prevent Blindness. We acknowledge the support of the Institute for Clinical and Translational Science (ICTS) at University of California Irvine (ULI TR001414/TR/NCATS).

References

Andersson G, et al. , 2003. On the origin of mitochondria: a genomics perspective. Phil. Trans. Roy. Soc. Lond. B Biol. Sci 358 (1429), 165–179. [PubMed: 12594925]

Asiabi P, et al. , 2020. Assessing and validating housekeeping genes in normal, cancerous, and polycystic human ovaries. J. Assist. Reprod. Genet 37 (10), 2545–2553. [PubMed: 32729067]

Barnhill AE, Brewer MT, Carlson SA, 2012. Adverse effects of antimicrobials via predictable or idiosyncratic inhibition of host mitochondrial components. Antimicrob. Agents Chemother 56 (8), 4046–4051. [PubMed: 22615289]

Beberok A, et al. , 2018. GSH depletion, mitochondrial membrane breakdown, caspase-3/7 activation and DNA fragmentation in U87MG glioblastoma cells: new insight into the mechanism of cytotoxicity induced by fluoroquinolones. Eur. J. Pharmacol 835, 94–107. [PubMed: 30086267]

Cavalier-Smith T, 2006. Origin of mitochondria by intracellular enslavement of a photosynthetic purple bacterium. Proc. Biol. Sci 273 (1596), 1943–1952. [PubMed: 16822756]

Dijk SN, et al. , 2020. Mitochondria as target to inhibit proliferation and induce apoptosis of cancer cells: the effects of doxycycline and gemcitabine. Sci. Rep 10 (1), 4363. [PubMed: 32152409]

Ding L, et al. , 2017. Joint toxicity of fluoroquinolone and tetracydine antibiotics to zebrafish (Danio rerio) based on biochemical biomarkers and histopathological observation. J. Toxicol. Sci 42 (3), 267–280. [PubMed: 28496033]

Duewelhenke N, Krut O, Eysel P, 2007. Influence on mitochondria and cytotoxicity of different antibiotics administered in high concentrations on primary human osteoblasts and cell lines. Antimicrob. Agents Chemother 51 (1), 54–63. [PubMed: 17088489]

Etminan M, et al. , 2012. Oral fluoroquinolones and the risk of retinal detachment. Jama 307 (13), 1414–1419. [PubMed: 22474205]

Falagas ME, Rafailidis PI, Rosmarakis ES, 2007. Arrhythmias associated with fluoroquinolone therapy. Int. J. Antimicrob. Agents 29 (4), 374–379. [PubMed: 17241772]

Glickman RD, 2002. Phototoxicity to the retina: mechanisms of damage. Int. J. Toxicol 21 (6), 473–490. [PubMed: 12537644]

Hangas A, et al. , 2018. Ciprofloxacin impairs mitochondrial DNA replication initiation through inhibition of Topoisomerase 2. Nucleic Acids Res. 46 (18), 9625–9636. [PubMed: 30169847]

Hollborn M, et al. , 2011. The human Müller cell line MIO-M1 expresses opsins. Mol. Vis 17, 2738–2750. [PubMed: 22065927]

Hooper DC, 2001. Mechanisms of action of antimicrobials: focus on fluoroquinolones. Clin. Infect. Dis 32 (Suppl. ment_1), S9–S15. [PubMed: 11249823]

Jiang D, et al. , 2019. Donation of mitochondria by iPSC-derived mesenchymal stem cells protects retinal ganglion cells against mitochondrial complex I defect-induced degeneration. Theranostics 9 (8), 2395–2410. [PubMed: 31149051]

Kalghatgi S, et al. , 2013a. Bactericidal antibiotics induce mitochondrial dysfunction and oxidative damage in Mammalian cells. Sci. Transl. Med 5 (192), 192ra85.

Kalghatgi S, et al. , 2013b. Bactericidal antibiotics induce mitochondrial dysfunction and oxidative damage in mammalian cells. Sci. Transl. Med 5 (192), 192ra85–192ra85.

Kalyanaraman B, et al. , 2012. Measuring reactive oxygen and nitrogen species with fluorescent probes: challenges and limitations. Free Radic. Biol. Med 52 (1), 1–6. [PubMed: 22027063]

Kanbay M, et al. , 2006. A rare but serious side effect of levofloxacin: hypoglycemia in a geriatric patient. Diabetes Care 29 (7), 1716–1717. [PubMed: 16801617]

Kenney MC, et al. , 2010. Characterization of retinal and blood mitochondrial DNA from age-related macular degeneration patients. Invest. ophthal. visual sci 51 (8), 4289–4297. [PubMed: 20357205]

Kohanski MA, et al. , 2007. A common mechanism of cellular death induced by bactericidal antibiotics. Cell 130 (5), 797–810. [PubMed: 17803904]

Kubrusly RC, et al. , 2008. Expression of functional dopaminergic phenotype in purified cultured Müller cells from vertebrate retina. Neurochem. Int 53 (3–4), 63–70. [PubMed: 18582514]

Lawrence JW, et al. , 1996. Delayed cytotoxicity and cleavage of mitochondrial DNA in ciprofloxacin-treated mammalian cells. Mol. Pharmacol 50 (5), 1178–1188. [PubMed: 8913349]

Limb GA, et al. , 2002. In vitro characterization of a spontaneously immortalized human Müller cell line (MIO-M1). Invest. Ophthalmol. Vis. Sci 43 (3), 864–869. [PubMed: 11867609]

Lobritz MA, et al. , 2015. Antibiotic efficacy is linked to bacterial cellular respiration. Proc. Natl. Acad. Sci. U. S. A 112 (27), 8173–8180. [PubMed: 26100898]

Lorenz L, et al. , 2021. Cell surface profiling of retinal müller glial cells reveals association to immune pathways after LPS stimulation. Cells 10 (3).

Mather R, et al. , 2002. Fourth generation fluoroquinolones: new weapons in the arsenal of ophthalmic antibiotics. Am. J. Ophthalmol 133 (4), 463–466. [PubMed: 11931779]

Mohammed HH, et al. , 2019. Current trends and future directions of fluoroquinolones. Curr. Med. Chem 26 (17), 3132–3149. [PubMed: 29446718]

Natoli R, et al. , 2017a. Microglia-derived IL-1β promotes chemokine expression by Müller cells and RPE in focal retinal degeneration. Mol. Neurodegener 12 (1), 31. [PubMed: 28438165]

Natoli R, et al. , 2017b. Microglia-derived IL-1β promotes chemokine expression by Müller cells and RPE in focal retinal degeneration. Mol. Neurodegener 12 (1), 31. [PubMed: 28438165]

Perry SW, et al. , 2011. Mitochondrial membrane potential probes and the proton gradient: a practical usage guide. Biotechniques 50 (2), 98–115. [PubMed: 21486251]

Roberts MC, 2019. Tetracyclines: mode of action and their bacterial mechanisms of resistance. Bacterial Resistance to ABacteri. Resis. Antibio. From Mol. Manntibiotics–From Molecules to Man 101–124.

Salamon SM, 1985. Tetracyclines in ophthalmology. Surv. Ophthalmol 29 (4), 265–275. [PubMed: 3157226]

Salimiaghdam N, et al. , 2020. Potential adverse effects of ciprofloxacin and tetracycline on ARPE-19 cell lines. BMJ Open Ophthalmol. 5 (1), e000458.

Samarakoon N, Harrisberg B, Ell J, 2007. Ciprofloxacin-induced toxic optic neuropathy. Clin. Exp. Ophthalmol 35 (1), 102–104. [PubMed: 17300586]

Sánchez AR, Rogers III RS, Sheridan PJ, 2004. Tetracycline and other tetracycline-derivative staining of the teeth and oral cavity. Int. J. Dermatol 43 (10), 709–715. [PubMed: 15485524]

Sandhu HS, et al. , 2016. Oral fluoroquinolones and the risk of uveitis. JAMA ophthalmol. 134 (1), 38–43. [PubMed: 26512796]

Sapadin AN, Fleischmajer R, 2006. Tetracyclines: nonantibiotic properties and their clinical implications. J. Am. Acad. Dermatol 54 (2), 258–265. [PubMed: 16443056]

Sarkar S, et al. , 2013. To compare the in vitro activity of 3 popular fluoroquinolones against common respiratory and middle ear pathogens. Bengal J. Otolaryngol. Head Neck Surg 21 (2), 18–21.

Sharma PC, Jain A, Jain S, 2009. Fluoroquinolone antibacterials: a review on chemistry, microbiology and therapeutic prospects. Acta Pol. Pharm 66 (6), 587–604. [PubMed: 20050522]

Shutter MC, Akhondi H, 2019. Tetracycline. In: StatPearls [Internet]. StatPearls Publishing.

Silver N, et al. , 2006. Selection of housekeeping genes for gene expression studies in human reticulocytes using real-time PCR. BMC Mol. Biol 7 (1), 33. [PubMed: 17026756]

Smilack JD, Wilson WR, Cockerill FR III, 1991. Tetracyclines, chloramphenicol, erythromycin, clindamycin, and metronidazole. In: Mayo Clinic Proceedings. Elsevier.

Smith A, et al., 2001. Fluoroquinolones. Drugs 61 (6), 747–761. [PubMed: 11398907]

Stevens SX, Fouraker BD, Jensen HG, 1991. Intraocular safety of ciprofloxacin. Arch. Ophthalmol 109 (12), 1737–1743. [PubMed: 1841587]

Thompson AM, 2007. Ocular toxicity of fluoroquinolones. Clin. Exp. Ophthalmol 35 (6), 566–577. [PubMed: 17760640]

Velez G, et al. , 2012. Retinal pigment epithelium and müller progenitor cell interaction increase müller progenitor cell expression of PDGFRα and ability to induce proliferative vitreoretinopathy in a rabbit model. Stem Cell. Int 2012, 106486.

Vila J, et al. , 1996. Detection of mutations in parC in quinolone-resistant clinical isolates of Escherichia coli. Antimicrob. Agents Chemother 40 (2), 491–493. [PubMed: 8834907]

Wagai N, Tawara K, 1992. Possible direct role of reactive oxygens in the cause of cutaneous phototoxicity induced by five quinolones in mice. Arch. Toxicol 66 (6), 392–397. [PubMed: 1332649]

Wallace I, et al. , 1989. The ocular hypotensive effects of demeclocycline, tetracycline and other tetracycline derivatives. Invest. Ophthal. Visual Sci 30 (7), 1594–1598. [PubMed: 2501230]

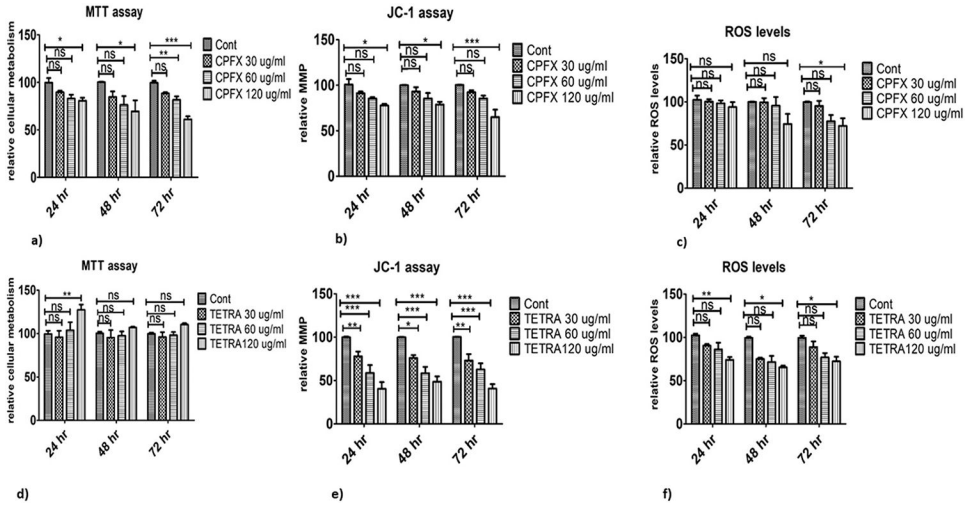

Fig. 1.

Treatment effects of CPFX and TETRA on metabolism, MMP and intracellular levels of ROS in MIO-M1 cells via MTT, JC-1 and ROS assays. (1a) Cellular metabolism declined by 120 μg/ml CPFX in 24 and 48 h, 60 and 120 μg/ml of CPFX in 72 h; (1d) increased cellular metabolism by 120 μg/ml TETRA in 24 h cultures; (1b) the lowest MMP with 120 μg/ml CPFX in all cultures; (1e) decreased MMP with 30, 60 and 120 μg/ml of TETRA in all incubation times; (1c) reduced levels of ROS in 72 h with 120 μg/ml of CPFX; (1f) significant decrease of ROS levels with 120 μg/ml of TETRA in all time periods. Cont stands for vehicle-control cells. (*P < 0.05, **P < 0.01, ***P < 0.0001).

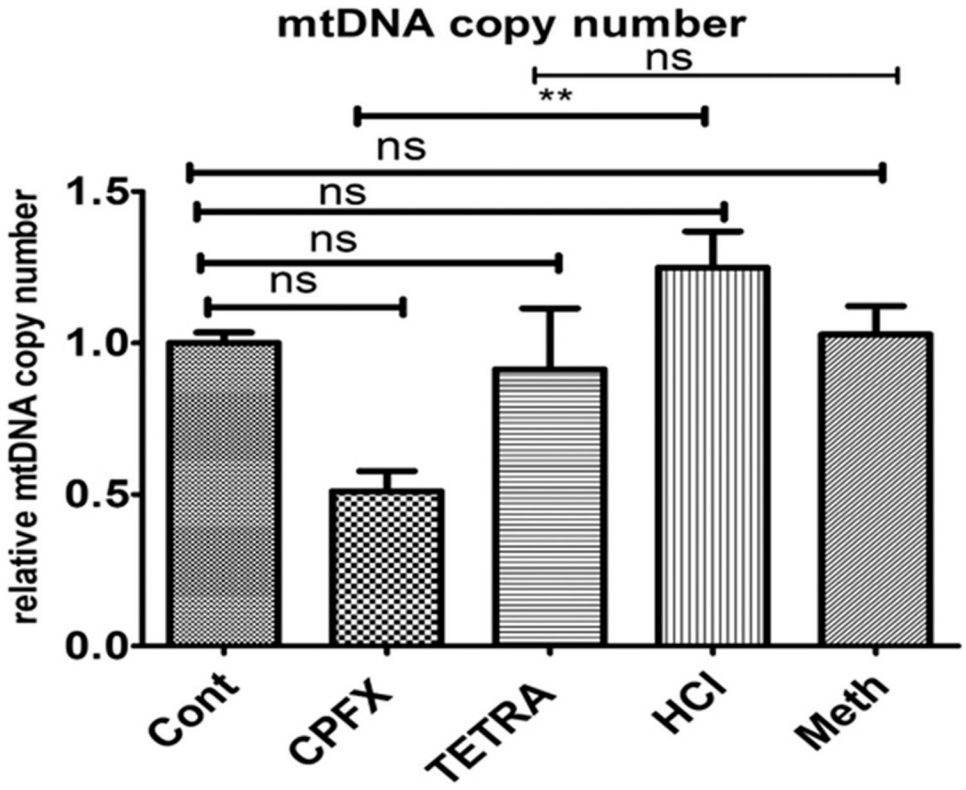

Fig. 2.

Effects of TETRA and CPFX on levels of mtDNA copy numbers. Significant reduction of mtDNA level by CPFX treatment; no effects of TETRA on mtDNA copy number. Cont represent untreated cells. (*P < 0.05, **P < 0.01, ***P < 0.0001).

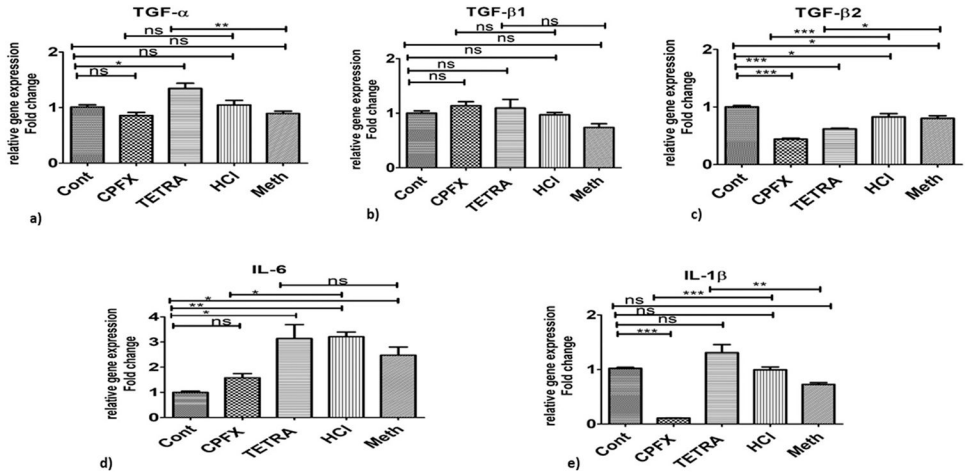

Fig. 3.

Altered expression levels of inflammatory pathway genes after treatment with CPFX and TETRA. Substantial higher expression levels of *TGF-α* (3a), and *IL-1β* (3e) in TETRA treated cultures. There were lower expression levels of *TGF-β2* in MIO-M1 cells treated by both antibiotics (3c). Lower expression of *IL-6* (3d) and *IL-1β* (3e) after treatment with CPFX; There were no effects of either treatments on *TGF-β1* gene expression levels (3b). Cont represents untreated cells. (*P < 0.05, **P < 0.01, ***P < 0.0001).

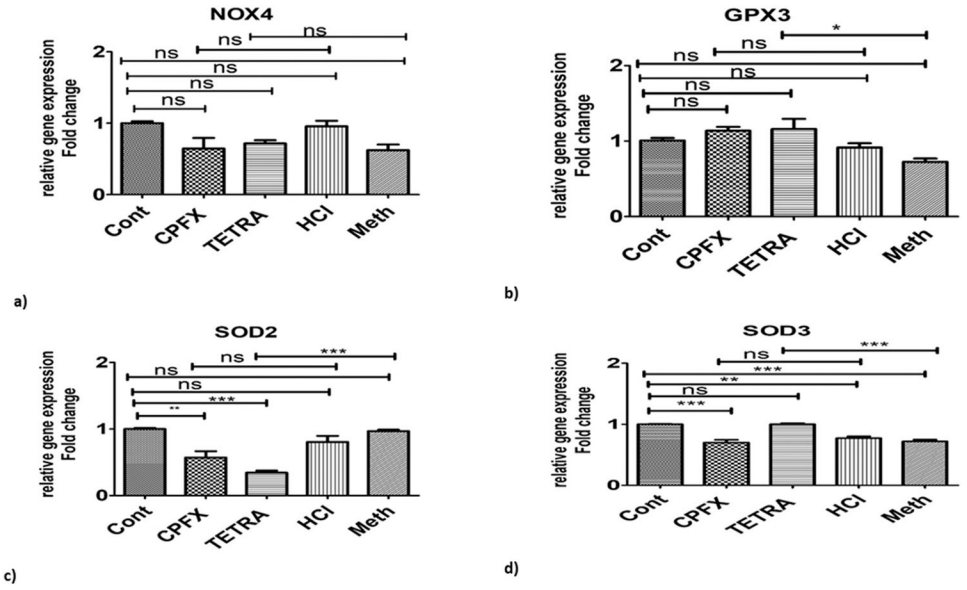

Fig. 4.

Effects of TETRA and CPFX on genomic expression of antioxidant pathway related enzymes. Higher expression levels of *GPX3* and *SOD3* enzymes were seen after TETRA treatment (4b and 4d). *SOD2* levels decreased after TETRA treatment (4c); and neither treatments affected *NOX4* gene expression levels (4a). Cont represents untreated cells. (*P < 0.05, **P < 0.01, ***P < 0.0001).

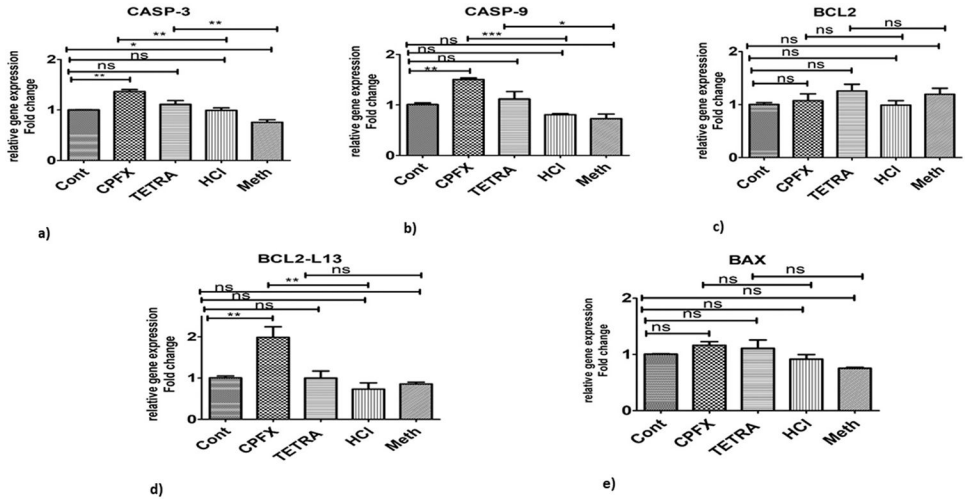

Fig. 5.

Altered expression levels of apoptotic pathway genes in CPFX and TETRA treated MIO-M1 cells. There were higher expression levels of *CASP-3* and *CASP-9* by both treatments (5a and 5b); elevated levels of *BCL2-L13* was induced by CPFX (5d); and there were no effects of CPFX and TETRA on *BCL2* (5c) and *BAX* gene expression levels (5e). Cont represents untreated cells. (*P < 0.05, **P < 0.01, ***P < 0.0001).

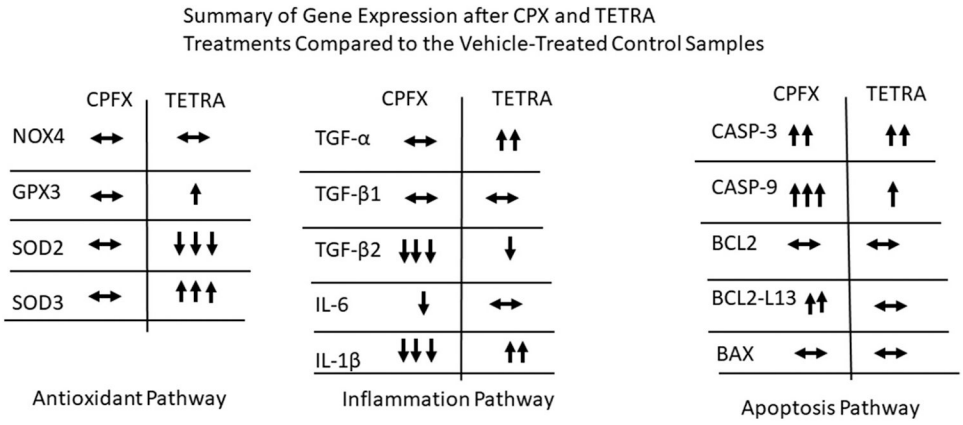

Fig. 6.

Summary of gene expression after CPFX and TETRA treatments compared to the vehicle-control samples.

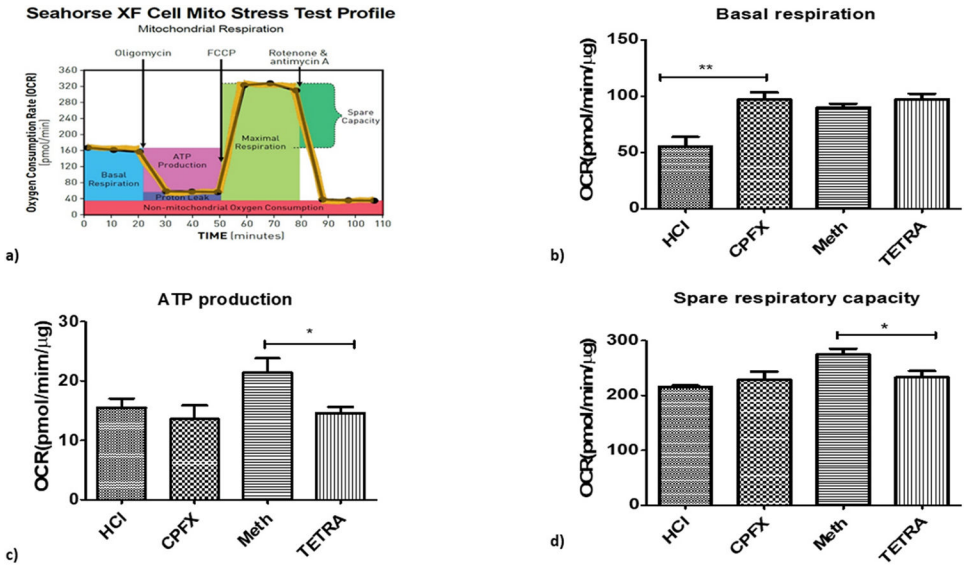

Fig. 7.

Impacts of CPFX and TETRA on the biogenetic profile and oxygen consumption rate (OCR). Higher OCR level in CPFX treated cells in basal condition (7b); lower level of ATP production (7c) and lower level of spare respiratory capacity (7d) in TETRA treated cells. (*P < 0.05, **P < 0.01, ***P < 0.0001).

Table 1

Information of the genes related to apoptotie, inflammatory and antioxidant pathways in MIO-M1 cells.

Symbol	Gene Name	GenBank Accession No.	Sigma Primer sequences Or Qiagen GeneGlobe ID	Function
BAX	BCL2 associated X	NM_001291429 NM_001291428 NM_001291430 NM_001291431 NM_004324 NM_138761 NM_138763 NM_138764	QT00031192	This gene encodes a mitochondrially-localized protein with conserved B-cell lymphoma 2 homology motifs. Higher expression of the encoded protein induces apoptosis.
BCL2L13	BCL2 like 13	NM_015367 NM_001270729 NM_001270731 NM_001270732 NM_001270734 NM_001270735	QT00093282	Encodes a mitochondrially-localized protein, apoptosis inducer
BCL2	BCL2 apoptosis regulator	NM_000633	QT00025011	Encodes an integral outer mitochondrial membrane protein that blocks the apoptotie death of some cells (e.g. lymphocytes).
CASP-3	caspase 3, apoptosis-related cysteine peptidase	NM_004346 NM_032991	QT00023947	Encodes protein as a cysteine-aspartic acid protease that plays a central role in the execution-phase of cell apoptosis.
CASP-9	caspase 9, apoptosis-related cysteine peptidase	NM_001229NM_032996	QT00036267	Encodes a member of the cysteine-aspartic acid protease (caspase) family, which is involved in the execution-phase of cell apoptosis.
IL-1β	interleukin 1, beta	NM_000576	FH1-5′-CTAAACAGATGAAGTGCTCC-3′ RH1-5′-GGTCATTCTCCTGGAAGG-3′	Produced by activated macrophages, IL-1 stimulates thymocyte proliferation. The protein encoded by this gene is a member of the interleukin 1 cytokine family. This cytokine is a pleiotropic cytokine involved in various immune responses, inflammatory processes, and hematopoiesis
IL-6	interleukin 6	www.ncbi.nlm.nih.gov/nuccore/M19154′/>NM_000600	FH1-5′-GCAGAAAAAGGCAAAGAATG-3′ RH1-5′-CTACATTTGCCGAAGAGC-3′	This gene encodes a cytokine that functions in inflammation and the maturation of B cells. In addition, the encoded protein has been shown to be an endogenous pyrogen capable of inducing fever in people with autoimmune diseases or infections
TGF-α	transforming growth factor alpha	NM_003236 NM_001099691	QT00033887	This gene encodes a growth factor that is a ligand for the epidermal growth factor receptor, which activates a signaling pathway for cell proliferation, differentiation and development. This protein may act as either a transmembrane-bound ligand or a soluble ligand.
TGF-β1	transforming growth factor beta-1-like	NM_003238	FH1-5′-AACCCACAACGAAATCTATG-3′ 5′-CTTTTAACTTGAGCCTCA-GC-3′ RH1-	This gene is a polypeptide member of the transforming growth factor beta superfamily of cytokines. It is a secreted protein that performs many cellular functions, including the control of cell growth, cell proliferation, cell differentiation, and apoptosis.
TGF-β2	transforming growth factor beta 2	NM_001135599	FH1-5′-CACTTACGTTCATTGACTCC-3′ RH1-5′-AAAAAACGACAGTCTAGTTGC-3′	This gene encodes a secreted ligand of the TGF-beta (transforming growth factor-beta) superfamily of proteins. Ligands of this family bind various TGF-beta receptors leading to recruitment and activation of SMAD family transcription factors that regulate gene expression.

Symbol	Gene Name	GenBank Accession No.	Sigma Primer sequences Or Qiagen GeneGlobe ID	Function
SOD2	superoxide dismutase 2	NM_000636	FH1-5′-ATCTACCCTAATGATCCCAG-3′ RH1-5′-AGGACCTTATAGGGTTTTCAG-3′	This gene is a member of the iron/manganese superoxide dismutase family. It encodes a mitochondrial protein that forms a homotetramer and binds one manganese ion per subunit. This protein binds to the superoxide byproducts of oxidative phosphorylation and converts them to hydrogen peroxide and diatomic oxygen.
SOD3	superoxide dismutase 3	NM_003102	QT01664327	This gene encodes a member of the superoxide dismutase (SOD) protein family, which catalyzes the conversion of superoxide radicals into hydrogen peroxide and oxygen, effective in protection of the brain, lungs, and other tissues from oxidative stress.
GPX3	glutathione peroxidase 3	NM_002084	FH1-5′-GCAACCAATTTGGAAAACAG-3′ RH1-5′-CTCAAAGAGCTGGAAATTAGG-3′	The protein encoded by this gene belongs to the glutathione peroxidase family, members of which catalyze the reduction of organic hydroperoxides and hydrogen peroxide (H2O2) by glutathione, and thereby protect cells against oxidative damage. Several isozymes of this gene family exist in vertebrates, which vary in cellular location and substrate specificity.
NOX4	NADPH oxidase 4	NM_001143836NM_016931 NM_001143837NR_026571 NM_001291926NM_001300995 XM_006718848 NM_001291927XM_006718852 XM_006718853NM_001291929 XM_006718849	FH1-5′-AATTTAGATACCCACCCTCC-3′ RH1-5′-TCTGTGGAAAATTAGCTTGG-3′	This gene encodes a member of the NOX-family of enzymes that functions as the catalytic subunit the NADPH oxidase complex. The encoded protein is localized to non-phagocytic cells where it acts as an oxygen sensor and catalyzes the reduction of molecular oxygen to various reactive oxygen species (ROS).
HPRT1	Hypoxanthine Phosphoribosyltransferase 1	NM_000194	FH1-5′-ATAAGCCAGACTTTGTTGG-3′ RH1-5′-ATAGGACTCCAGATGTTTCC-3′	The protein encoded by this gene is a transferase, which catalyzes conversion of hypoxanthine to inosine monophosphate and guanine to guanosine monophosphate via transfer of the 5-phosphoribosyl group from 5-phosphoribosyl 1-pyrophosphate. This enzyme plays a central role in the generation of purine nucleotides through the purine salvage pathway.